Proceedings of the ASME 2012 Summer Heat Transfer Conference
HT2012
July 8-12, 2012, Rio Grande, Puerto Rico

HT2012-58379

EFFECTS OF GEOMETRICAL PARAMETERS ON NATURAL CONVECTIVE HEAT TRANSFER FROM VERTICALLY-MOUNTED RECTANGULAR INTERRUPTED FINS

Golnoosh Mostafavi
MASc Candidate, Laboratory for Alternative Energy Conversion (LAEC), Mechatronics System Engineering, SFU
Surrey, British Columbia, Canada

Mehran Ahmadi
PhD Candidate, Laboratory for Alternative Energy Conversion (LAEC), Mechatronics System Engineering, SFU
Surrey, British Columbia, Canada

Majid Bahrami*
Associate Professor, Laboratory for Alternative Energy Conversion (LAEC), Mechatronics System Engineering, SFU
Surrey, British Columbia, Canada

ABSTRACT

Steady-state external natural convection heat transfer from vertically-mounted rectangular interrupted fins is investigated numerically and experimentally. To perform an experimental study, a custom-designed testbed was developed to verify the analytical and numerical results. FLUENT software was used in order to develop a 2-D numerical model for investigation of interruption effects and performing parametric study. After regenerating, and validating the existing analytical results for fin spacing, a systematic numerical and experimental study was conducted on effect of fin interruption. Results show that adding interruptions to vertical rectangular fins enhances the thermal performance of fins. In a parametric study optimum interruption length for maximum fin performance was found and correlated.

1. INTRODUCTION

Passive cooling is a widely preferred method for electronic and power electronic devices since it is a low price, [1]quiet, and trouble free solution. Air-cooling is recognized as an important technique in the thermal design of electronic packages, because its accessibility particularly with respect to safe operation in hostile environments (contaminated air, vibrations, noise, and humidity) [1]. These features stimulated considerable research on the development of optimized finned heatsinks and enclosures [2-6]. Natural convective heat transfer form vertical rectangular fins, and also pin fins is a well-established subject in the literature. It has been investigated analytically, numerically and experimentally. The following paragraphs provide a brief overview on the pertinent literature; the previous studies are grouped into analytical, numerical, and experimental works, more detailed reviews can be found elsewhere [7].

1.1. Analytical approach: Pioneering analytical work in this area was carried out by Elenbaas [8]. He investigated isothermal finned heatsink analytically and experimentally. The analytical study resulted in general relations for natural convective heat transfer from vertical rectangular fins that is not accurate for small values of fin spacing. Churchil [9] developed a general correlation for the heat transfer rate from vertical channels using the theoretical and experimental results obtained by a number of authors. Bar-Cohen and Rohsenow [10] also performed an analytical study to investigate the natural convective heat transfer from two parallel plates. They developed a relationship for Nusselt number in terms of Rayleigh number for isothermal and isoflux plates. They also reported a correlation for the optimum fin spacing.

$$Nu_s = \frac{h\,s}{k} = \left[\frac{576}{\left(\frac{Ra_s s}{L}\right)^2} + \frac{2.873}{\left(\frac{Ra_s s}{L}\right)^{0.5}}\right]^{-0.5} \quad (1)$$

Where Ra_s is Rayleigh number based on fin spacing, s is the fin spacing between two adjacent fins, L is length of the fins, h

* Corresponding author. Fax: +1 7787827514.
E-mail address: mbahrami@sfu.ca

is convective heat transfer coefficient and k is thermal conductivity. Please see Fig. 1. Another relation was introduced by Culham *et al.* [11] for characteristic length scale based on the squared root of the wetted area.

1.2. Numerical approach: Bodoia and Osterle [12], followed Elenbaas [8] and used a numerical approach to investigate developing flow in the channel and heat transfer between symmetrically heated, isothermal plate in an effort to predict the channel length required to achieve fully developed flow as a function of the channel width and wall temperature. Ofi and Hetherington [13] used a finite element method to study the natural convective heat transfer from open vertical channels. Culham *et al.* [11] also used a numerical code[2] to simulate the free convective heat transfer from a vertical fin array.

1.3. Experimental approach: Several experimental works in this area was carried out. Starner and McManus [14], Welling and Wooldridge [15], Chaddock [16], Aihara [17, 18], Leung *et al*. [19–25] and Van de Pol and Tierney [26] are some examples, which were mostly focused on the effects of varying fin geometric parameters, the array, and base plate orientation.

Radiation heat transfer plays an important role in the heat transfer from fin arrays. This has been shown by Edwards and Chaddock [27], Chaddock [28], Sparrow and Acharya [29], Saikhedkar and Sukhatme [30], Sparrow and Vemuri [31, 32], Azarkish*et al*. [33], and Rao *et al*. [34]. It has been reported that the radiation heat transfer contributes between 25–40% of the total heat transfer from fin arrays in naturally cooled heatsinks. A summary of the above-mentioned studies is presented in Table 1.

Our literature review suggests that the focus of the literature has been mostly on continuous fins and pin fins, and no in-depth study has been performed to investigate the natural convection heat transfer from interrupted fins for external natural convective heat transfer. As such, in this paper, we aim at investigating the effect of fin interruption. Interrupted fins are more general form of fins and can include both continuous and pin fins (Fig. 1). In a closer look, continuous fins and pin fins are two limiting cases of the targeted interrupted fins. A proper selection of fin spacing and interruption sizes can lead to higher thermal performance. This is a direct result of thermal boundary layer interruption. Furthermore, fin interruption leads to significant weight and thus cost reductions in heatsinks. The goal of this study is to investigate the effects of adding interruption to fins and determine an optimum value for different geometrical parameters of the fin array, mainly the length of fin interruption.

NOMENCLATURE

A	Surface area, m^2
g	Gravitational acceleration, m^2/s
G	Fin interruption length, m
h	Convection heat transfer coef. W/m^2K
H	Fin height, m
I	Electrical current, A
k	Thermal conductivity, W/mK
l	Fin length, m
L	Enclosure length, m
n	Number of interruptions
N	Number of fins per row
Nu	Nusselt number
P	Pressure,Pa
P_{input}	Input power, W
Pr	Prandtl number
Q	Heat transfer rate, W
Ra	Rayleigh number
s	Fin spacing, m
t	Fin thickness, m
T	Temperature, K
u	Flow velocity in x direction, m/s
v	Flow velocity in y direction, m/s
V	Electrical voltage, V
W	Enclosure width, m
x	Direction normal to fin surface, m
y	Direction along fin surface, m

Greek symbols

α	Exponent in Archie's law
β	Coefficient of volume expansion, $1/K$
μ	Fluid viscosity, Ns/m^2
ρ	Density, kg/m^3

Subscripts

atm	atmosphere
opt	Optimum

[2]META

Table 1: Summery of literature review

Author	Method	Variations	*Ra* number range	Correlation
Elenbaas [8]	Analytical and Experimental	Fin spacing Temperature difference	$10^{-1}-10^{5}$	$Nu_s=\frac{1}{24}Ra_s\left[1-\exp\left(-\frac{35}{Ra_s}\right)\right]^{\frac{3}{4}}$
Bar-Cohen and Rohsenow [10]	Analytical		*all*	$Nu_s=\left[\left(\frac{24}{Ra_s}\right)^2+\left(\frac{1}{0.59\,Ra_s^{0.25}}\right)^2\right]^{-0.5}$
Culham *et al.* [11]	Analytical and Numerical	Enclosure type(finned, bare)	$10^{-6}-10^{10}$	
Bodoia and Osterle [12]	Numerical			$Nu_s=\frac{1}{24}Ra_s$
Leung *et al.*[24]	Experimental		Ra<10^6	$Nu_s=0.135\,Ra_s^{0.5}$ Ra<250 $Nu_s=0.423\,Ra_s^{\frac{1}{3}}$ 250<Ra<10^6
Leung *et al.*[24]	Experimental		Ra<10^6	$Nu_s=0.144\,Ra_s^{0.5}$ Ra<250 $Nu_s=0.490Ra_s^{\frac{1}{3}}$ 250<Ra<10^6
Guvenc and Yuncu [4]	Experimental	Fin spacing Fin height Temperature difference	$10^6-6\times10^6$	

2. PROBLEM STATEMENT

A schematic of the considered fin geometry along with the salient geometric parameters is shown in Fig. 1.

When a heatsink is heated, thermal boundary layers start to develop at the bottom edges of the opposing surfaces of the neighboring fins; the boundary layers eventually merge if the fins/channels are sufficiently long creating fully developed channel flow [35]. Interrupted fins disrupt the thermal boundary layer growth, maintaining a thermally developing flow regime, which in turn leads to a higher natural heat transfer coefficient.

The effect of fin interruption is investigated using a 2-D numerical simulation implementing FLUENT [38], in this study. In order to investigate the effects of fin interruption and to determine an optimum fin length to fin interruption ratio, we started by using the existing analytical models of [10, 36] to calculate the optimum fin spacing, *s*. The idea is to decouple the effect of fin spacing from the fin interruption. As such, the fin spacing will be kept constant at its optimum value calculated by Rosenhow-Bar-Cohen model [10], throughout the analysis.

3. GOVERNING EQUATIONS

The model consisted of the external natural convection heat transfer from a single channel. The conservation of mass, momentum and energy in the fluid are based on assuming a fluid with constant properties and the Boussinesq approximation [35] for density-temperature relation.

$$\frac{\partial u}{\partial x}+\frac{\partial v}{\partial y}=0 \tag{2}$$

$$\rho\left(u\frac{\partial u}{\partial x}+v\frac{\partial u}{\partial y}\right)=-\frac{\partial P}{\partial x}+\mu\nabla^2 u \tag{3}$$

$$\rho\left(u\frac{\partial v}{\partial x}+v\frac{\partial v}{\partial y}\right)=-\frac{\partial P}{\partial y}+\mu\nabla^2 u-\rho g \tag{4}$$

$$\left(u\frac{\partial T}{\partial x}+v\frac{\partial T}{\partial y}\right)=\alpha\nabla^2 T \tag{5}$$

Isothermal boundary conditions have been assumed on the walls, i.e.,$T=T_s$ at $x=\mp\frac{s}{2}, 0<y<l$, symmetry boundary condition for the interruption region $\frac{dT}{dx}=0$ at $x=\mp\frac{s}{2}$, $l<y<l+G$. And pressure inlet and outlet boundaries $P=P_{atm}$ at $y=L, y=0$ are the considered boundary conditions.

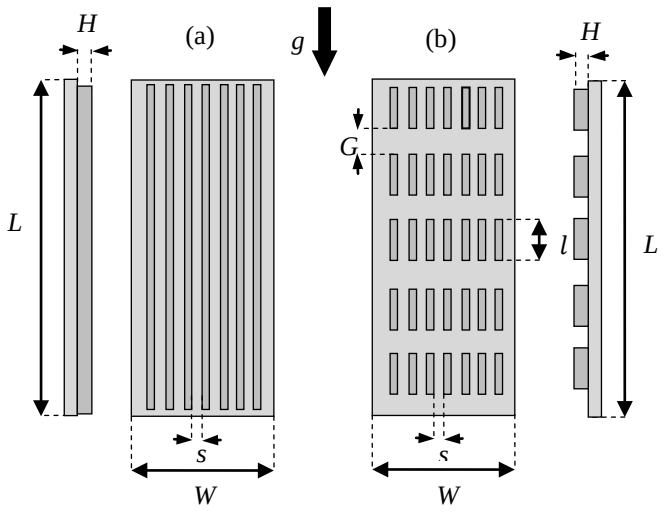

Figure 1: Schematic of the considered heatsink geometry, a) continuous rectangular finned heatsink; b) interrupted rectangular finned heat sink

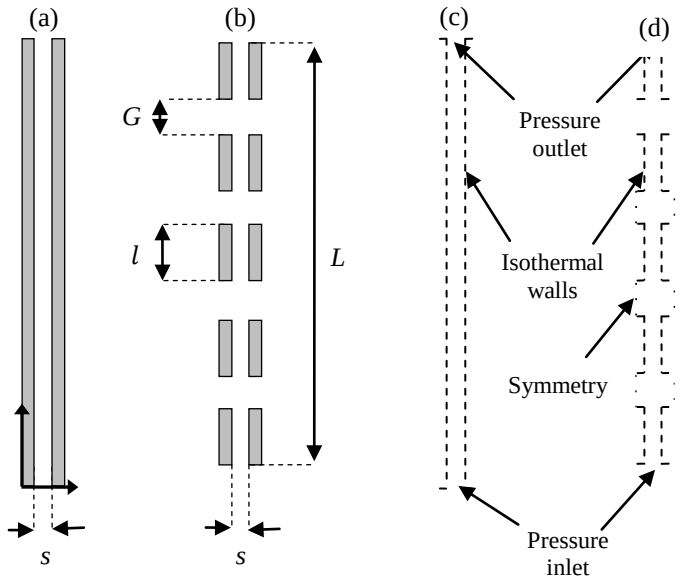

Figure 2: schematic of the numerical domain, a) continuous fins, b) interrupted fins; c) boundary conditions for continuous fins, d) boundary conditions for interrupted fins.

4. NUMERICAL APPROACH

A steady state 2-D model was developed in FLUENT [38] in order to investigate the effects of fin interruption on natural convective heat transfer from the fins. Because the geometry repeats itself, a single channel has been chosen to represent the computational domain (Fig. 2). According to flow visualization and velocity measurement of the flow field for a finned plate [37], the fresh air inflow, and outflow from the open side of the channels made by two neighboring fins was comparatively small. Accordingly, the influence of the side fins exposed to the ambient is not expected to be significant; therefore, the selection of a single channel instead of whole domain is a reasonable assumption. Also the influence of the flow in the direction normal to the base plate was shown to be negligible [37]. Therefore, a 2-D analysis (instead of 3-D) is a reasonable assumption. For the domain dimension selection the optimum fin spacing, *s*, is estimated using existing analytical models of [9, 36]. The effect of fin spacing was decoupled in simulation of interruptions in interrupted fins, keeping the fin spacing constant at its optimum value. The pressure inlet boundary condition is applied to the channel inlet (the bottom of the channel) which defines the static/gauge pressure at the inlet boundary. This is interpreted as the static pressure of the environment from which the flow enters. For the top of the domain, i.e. the outlet of the channel, outlet boundary condition is applied in which the flow direction should be defined. The symmetry boundary condition was chosen for the interruption region, which is equivalent to no heat flux in the direction normal to the fins surface plane. A no-slip isothermal solid surface is considered for the walls. Figure 2 shows a schematic of the domain considered for the numerical simulation, along with the chosen boundary conditions for continuous and interrupted fins.

For solving the system of partial differential equations explained in Section 3, ANSYS-Fluent 12.1.4 [38] have been employed, GAMBIT 2.3.16 was used for mesh generation. Boundary layer mesh has been used for the regions close to fin surface, in order to capture the flow behavior with higher resolution. Figure 3 shows a part of the domain and the generated mesh for continuous and interrupted fins. Grid independency study has performed for a continuous fin case, with seven different grid sizes in the *y*-direction, and four different grid sizes in the *x*-direction. Figure 4 shows the results for grid independency study along and normal to the fins, respectively. The optimum size for vertical grids has chosen to be 1 *mm*. Also 50 grids have been used in the horizontal space between two fin surfaces

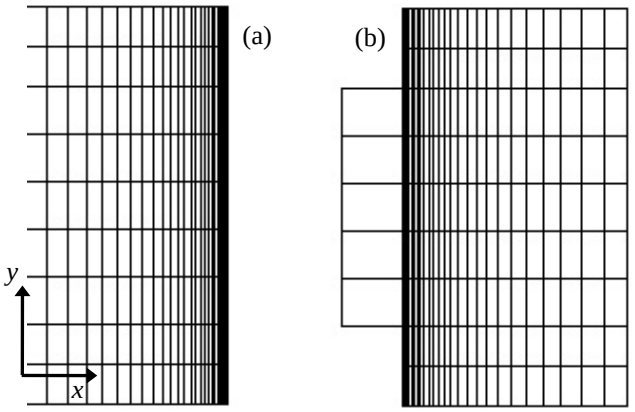

Figure 3: Grid used in the model for a) continuous and b) interrupted fins

Figure 5 shows the validation of the numerical simulation. Results for a continuous fin channel are compared to our experimental data and the analytical model of [10]. Figure 6 shows the results for both continuous and interrupted fins. As it

can be seen, there is a good agreement between numerical simulation results and both analytical and experimental results.

In Figs 5 and 6, the shown measured temperatures have been averaged to calculate a wall temperature for the experimental data. In Fig. 6 the heat transfer from the base plate is calculated and deduced from the total heat transfer rates to only consider the heat transfer from the fins. In addition, the radiation heat transfer (which can be as high as 40% [36]) has been removed from the data.

Table 2: Geometrical dimensions of the considered interrupted fins in numerical analysis

Considered numerical Geometry	*G/l*	*t* (*mm*)	*s* (*mm*)
1-5	0.5	2.5	9.5
6-10	1	2.5	9.5
11-15	2	2.5	9.5
16-20	5	2.5	9.5
21-25	10	2.5	9.5
26-28	20	2.5	9.5
29-32	40	2.5	9.5
33-35	80	2.5	9.5
36	255	2.5	9.5

Fin length and fin width is constant in all the geometries, L = 1.4*m* and s = 9.5*mm*.

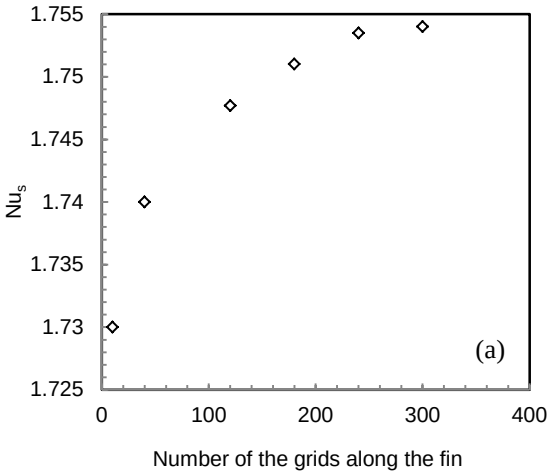

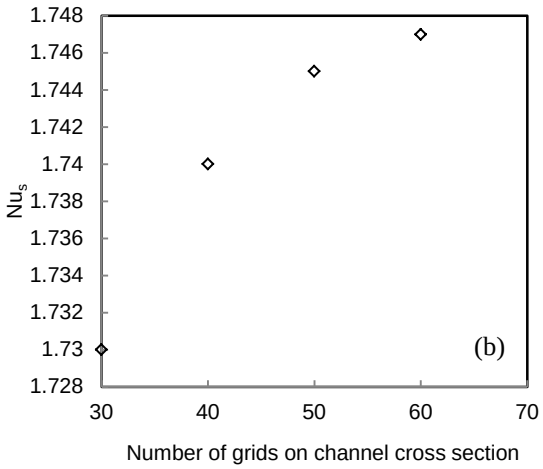

Figure 4: Grid independency study, *Ra* = 1.6E+3; a) in vertical direction (horizontal grids = 50); b) in horizontal direction (vertical grids =300)

Table 2 shows the specifications of the numerical domain geometry. Fin length and the interruption length have been changed respectively from $l = t, 2t, 5t, 10t, 15t$, where t is the fin thickness, and $G = l/2, l, 2l, 5l, 10l$ and in some cases $20l$, $40l$ and $80l$ or $225l$ Thirty six different geometries have been investigated overall.

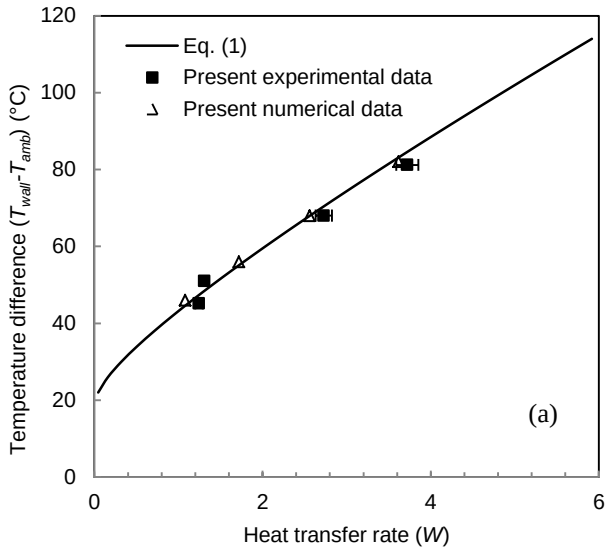

Figure 5: Numerical simulation validation; continuous fin, single channel (*s* = 9.5*mm*, *L* = 305*mm*, *H* = 17*mm*);

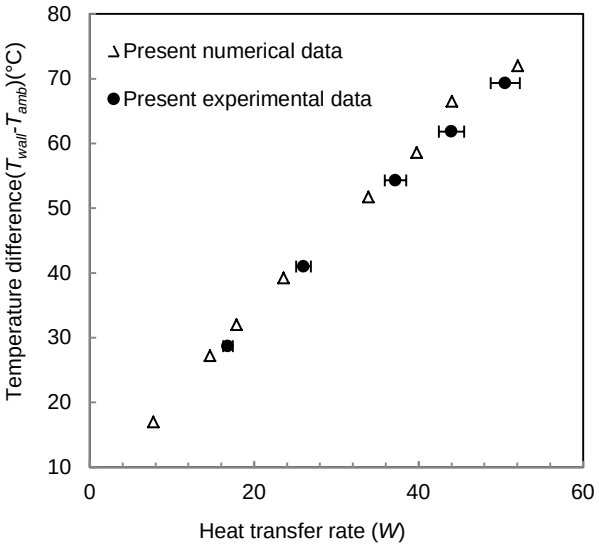

Figure 6: Numerical simulation validation; b) interrupted finned heatsink (n = 8, s = 9.5mm, L = 305mm, H = 17mm, l = 37mm, G = 30mm)

5. EXPERIMENTAL STUDY

The objective of the experimental work is to investigate the effects of fin spacing as well as the fin interruption length in rectangular fins. As such, two sets of heatsinks were prepared and tested featuring: i) continuous rectangular and ii) interrupted rectangular fins. Base plate dimensions of the samples were the same, but the number and dimensions of the fins were different as listed in Table 3 and Table 4.

5.1 THE TESTBED

The tested heatsinks were made from 6063-T5 aluminum alloy with thermal conductivity of 130 W/mK at 20℃ and emissivity ~0.8at20℃.A new testbed has been designed for measuring natural convection heat transfer from heatsinks as shown schematically in Fig. 7. The set-up included an enclosure made of Polymethylmethacrylate (PMMA) which was insulated by a layer of foam with thickness of 15 *mm*. The testbed also included a power supply, electrical heaters which were attached to the backside of the fins base-plate, and a DAQ system; thermal paste was used to decrease the thermal contact resistance between the heater and the heatsink base plate.

During the experiments the power input supplied to the heater and surface temperatures were measured at various locations at the back of the base-plate. Electrical power was supplied through an AC power supply (Transformer 10C) from Superior Electric (Ohio). The voltage and the current were measured to determine the power input to the heater. Five self-adhesive T-type copper-constantan thermocouples with accuracy of ± 1°C are installed in various locations on the surface of the enclosures, see Fig. 7b. All thermocouples are adhered to the inside surface of the enclosure to prevent disturbing the buoyancy-driven air flow. An additional thermocouple is used to measure the ambient room temperature during the experiments. Thermocouples are plugged into a TAC80B-T thermocouple-to-analog converter supplied by Omega (Toronto, ON). Temperature measurements were performed at five points in order to monitor the temperature variation over the heatsink. The average of these five readings was taken as the base plate temperature. Since fin heights are short (maximum fin height was 25 *mm*), fins were assumed to beisothermal.For each of the 12 heatsinks, the experimental procedure was repeated for power inputs 16, 25, 36, 42.2 and 49 *W*. The base-plate temperatureT_W, the ambient temperature T_∞, and the power input to the heater $\dot{Q}$; were recorded at steady-state, (The temperature was recorded and reaching 95% of the maximum temperature was considered steady-state) which lasted 100 minutes.

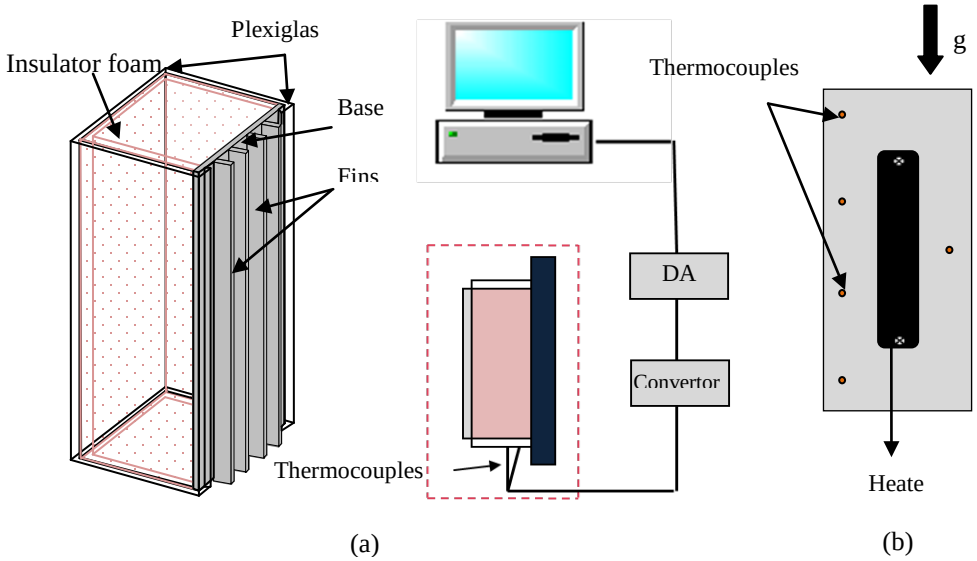

Figure 7: Schematic of the test-bed

Table 3: Dimensions of the finned plate samples; continuous fins, see Fig. 1a

Sample name	s (mm)	N	H (mm)	l (mm)
Cont-1-10-17	9.5	8	17	-
Cont-1-6-17	6.0	12	17	-
Cont-1-14-17	14.0	6	17	-
Cont-1-10-10	9.5	8	10	-
Cont-1-10-25	9.5	8	25	-

Table 4: Dimensions of finned plate samples; interrupted fins, see Fig. 1b

Sample name	s (mm)	N	H (mm)	l (mm)	n (number of interruptions)	G (mm)
Int-1-20	9.5	8	17.4	142.5	1	20
Int-2-20	9.5	8	17.4	88.3	2	20
Int-3-20	9.5	8	17.4	61.3	3	20
Int-4-20	9.5	8	17.4	45.0	4	20
Int-5-20	9.5	8	17.4	34.2	5	20
Int-4-20	9.5	8	17.4	37.0	4	30
Int-4-20	9.5	8	17.4	29.0	4	40

Fin base length and width are constant in all the samples, L = 305 *mm* and W= 101 *mm*.

5.2 UNCERTAINTY ANALYSIS

As given by Eq. (7), V and I are the electrical parameters measured in our experiments. The total accuracy in our measurements is evaluated according to the accuracy of the employed instruments. The accuracy of voltage and current readings are $1V$ and $0.01A$, respectively (Extech® 430 multimeter). The mentioned accuracy values are given with respect to the instruments readings, and not the maximum value of the readings. The maximum uncertainty for the measurements can be calculated from the following [39]. Maximum uncertainty value was called 3.5%. The calculated uncertainties are reported as error bars in the experimental results.

$$P_{input} = V.I \tag{7}$$

$$\frac{dP_{input}}{P_{input}} = \sqrt{\left(\frac{dV}{V}\right)^2 + \left(\frac{dI}{I}\right)^2} \tag{8}$$

6. RESULTS AND DISCUSSIONS

The effects of important parameters on the steady state natural convection heat transfer from interrupted rectangular fins are investigated. The effects of fin spacing, s, fin height, H for continuous fins and interruption length, G,on the average wall temperature are discussed in detail in the following subsections. The convective heat transfer from the fin arrays was studied for a range of each parameter, while the other geometric parameters were kept constant.

In order to verify the numerical results, 7 different interrupted finned heatsinks were studied experimentally. The averaged surface temperature was measured for various heat dissipation rates. The average surface temperature was also calculated using the existing relationships for natural convection and radiation heat transfer; please see Section 1 for more detail.

6.1 CONTINUOUS FINNED HEATSINKS

In the experimental study, 5 different continuous finned plates were investigated and the results were compared to the analytical existing model, Eq. (1). Adding the effect of radiative heat transfer to the existing analytical solutions, the optimum value of fin spacing for continuous rectangular fins were calculated. Heat transfer rates from heatsinks are plotted as a function of average wall temperature for fin length $L = 305mm$, fin spacing,$s = 6.0, 9.5,$ and $14.0mm$, and fin height $H = 10, 17, and\ 25mm$ in Figs. 8 and 9. As it was expected, the heat transfer rate from heatsinks depends on fin height, fin spacing and wall temperature; it is increasing with an increase in fin height and wall temperature. Heat transfer rates measured from three different fin heights are close to each other at low wall temperature, where at higher wall temperatures ($T_{wall} \approx 100℃$), the heat transfer rates tend to diverge, please see Fig. 9. As it can be seen, the experimental data and analytical solution

are in good agreement. To calculate the total heat transfer from the heatsink the convective heat transfer is calculated from Eq. (1) and heat transfer from base plate and radiation heat transfer are also added.

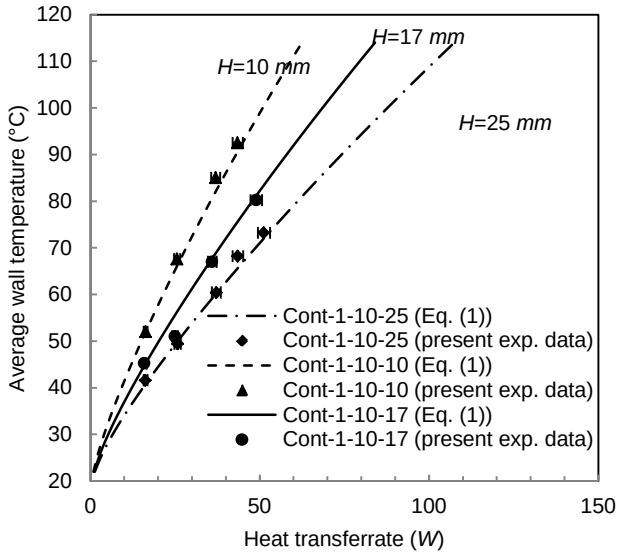

Figure 9: Comparison of the experimental data with theoretical predictions (Eq. 1) for different fin heights-continuous finned heatsinks

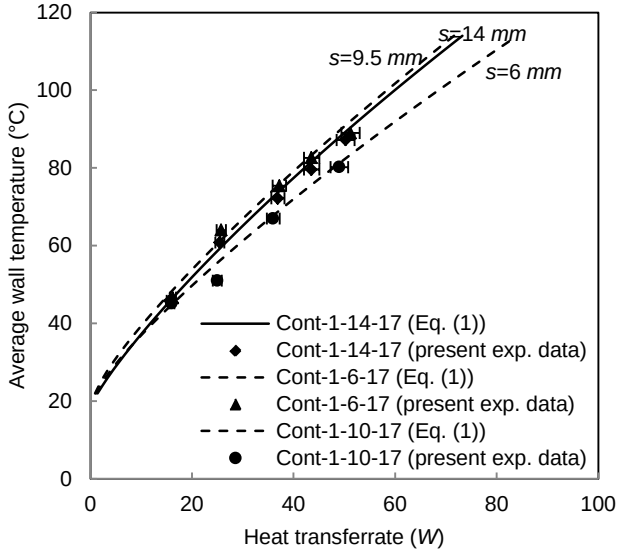

Figure 8: Comparison of the experimental data with theoretical predictions for different fin spacing-continuous finned heatsinks

6.2 EFFECT OF FIN SPACING

Heat transfer rate and mass of the heatsink are plotted as a function of fin spacing in Fig. 10. The figures were prepared for fin lengths $L = 305\ mm$, fin heights $H = 17\ mm$ and fin spacings, $s = 6, 9.5,$ and $14\ mm$, while the power input to the heater was kept constant at, $P_{input} = 40\ W$. As it is shown in Fig. 10, there is an optimum fin spacing to maximize the heat transfer rate for different average surface temperatures. It should be noted that the present experimental data are in good agreement when compared against the Analytical and experimental results reported by Bar-Cohen and Rohsenow [10] and Tamayol *et al.* [36], for optimum fin spacing.

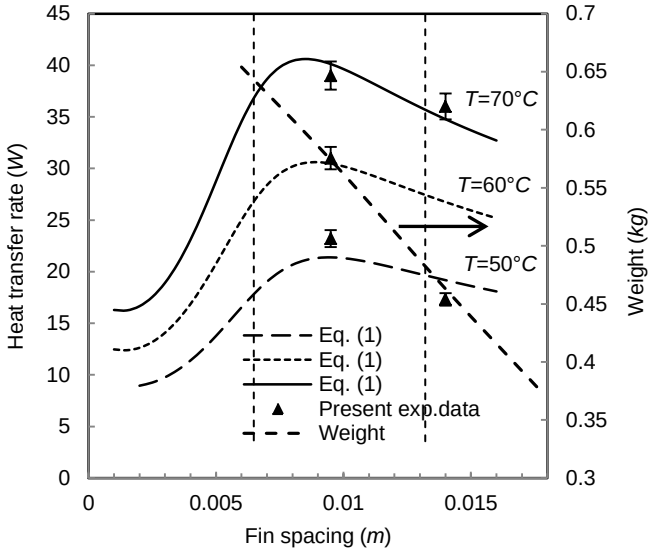

Figure 10: Heat transfer rate versus fin spacing for different average surface temperatures, fin base lengths $L = 305\ mm$, heights $H = 17\ mm$

6.3 EFFECTS OF FIN INTERRUPTION

Heat flux from heatsinks with interrupted fins is plotted in Figs. 11 and 12 as a function of average wall temperature for fin length $L = 305mm$, fin spacing $s = 9.5mm$, and fin height $H = 17mm$. Figure 11 shows the effect of interruption length. In this case four interruptions are made along the fin array and the interruption length was varied for $G = 20, 30$ and $40mm$. As it was expected heat flux improves as G increases. In Fig. 12 the effect of number of interruptions is investigated; the interruption length was kept constant at $20mm$, and $1, 2, 3, 4,$ and 5 interruptions were added to the fins. Both Figs. 11 and 12 show experimental data and numerical results.

Figure 13 shows the results of numerical simulation for the effect of fin interruption on the heat transfer from the fins. The interruption sizes are started from zero, which represents continuous fins. As it can be seen from Fig. 13 that:

- There is an optimum interruption length that maximizes the total heat transfer from the heatsink.
- It is a function of surface temperature and fin length. The optimum interruption length is correlated for different lengths and fin surface temperatures for $2.5mm < l < 25mm$ as follows:
- The proposed correlation is successfully predicting the maximum points on the curves for heat transfer rate.

$$\left(\frac{G}{l}\right)_{\text{Opt.}} = 8100(T_W - T_\infty)^{-2.2} \quad (9)$$

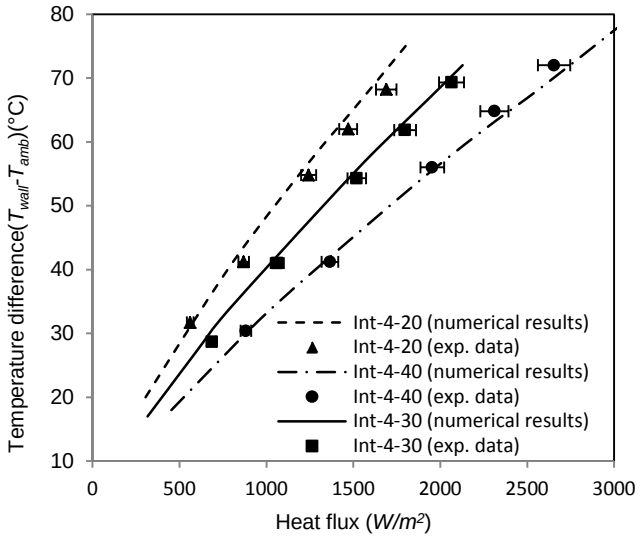

Figure 11: Experimental data and numerical results for different interruption lengths (20,30 and 40*mm*), *n* = 4,interrupted finned heatsinks

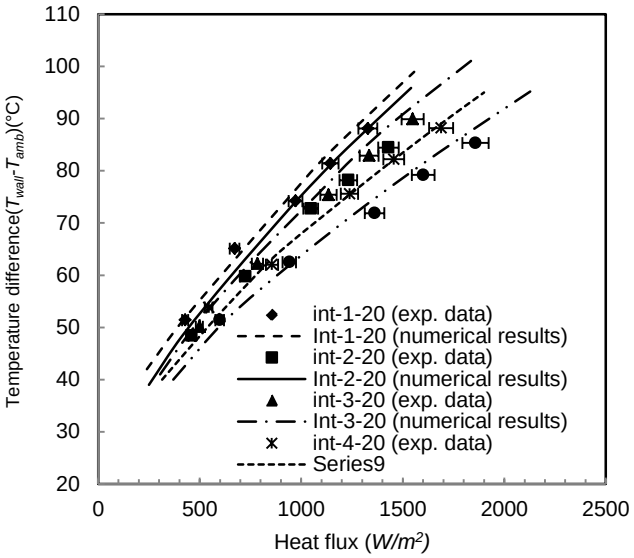

Figure 12: Experimental data and numerical results for different number of interruptions(1 , 2, 3, 4, and 5), *G* = 20*mm*, interrupted finned heatsinks

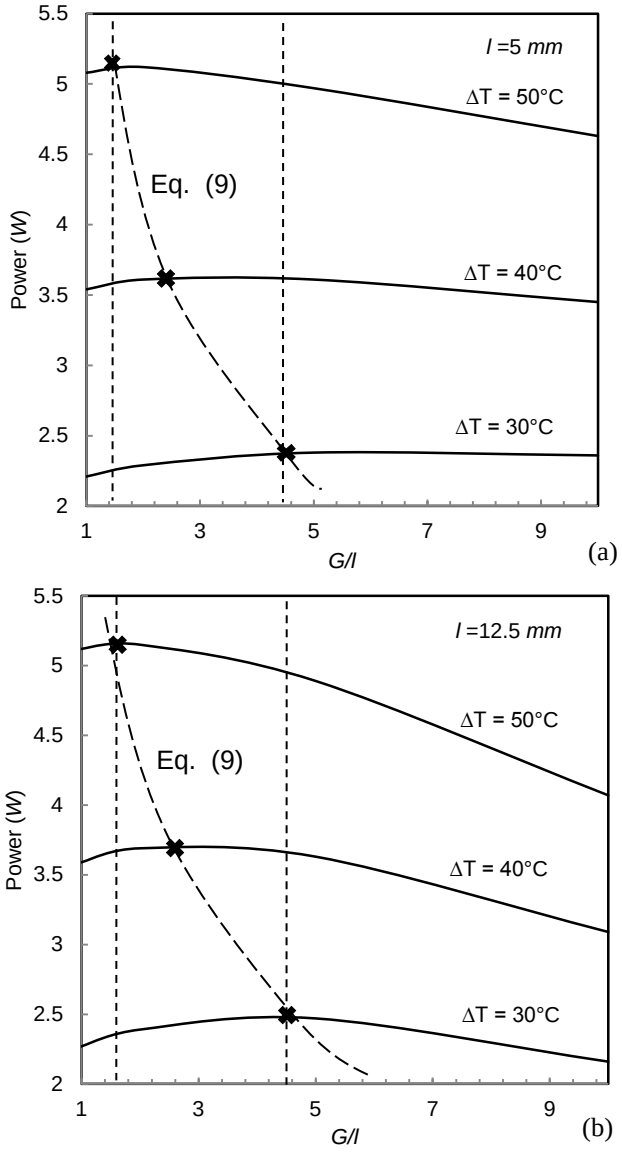

Figure 13: Effect of interruption length on total natural convection heat transfer from the heatsink (numerical results), a) fin length *l* = 5*mm*, and b) fin length *l* = 12.5*mm*

CONCLUSION AND SUMMERY

Experimental, numerical and analytical approached were employed in order to find the optimized geometrical fin parameters. Numerical and analytical results were verified by experimental data, and optimum fin spacing was calculated and compared to existing data in literature. A great consistency was observed. In a novel approach, interruptions were added to continuous fins with initial idea of resetting the hydrodynamic and thermal boundary layer in order to decrease thermal resistance. Experimental and numerical results show an increase in heat flux from the heatsink. Parametric studies showed an optimum interruption length which caused maximum heat transfer from the heatsink. This optimum heat

interruption length was also correlated and reported. In summary:

- There is an optimum interruption length that maximizes the total heat transfer from the heatsink.
- It is a function of surface temperature and fin length. The optimum interruption length is correlated for different lengths and fin surface temperatures for $2.5mm < l < 25mm$ as follows:
- The proposed correlation is successfully predicting the maximum points on the curves for heat transfer

REFERENCES

[1] Chu, Recent development of computer cooling technology, Keynote Paper, 6th International Symposium Transport Phenomena Thermal Engineering (ISTP-6), (1993).

[2] Yuncu, Anbar, An experimental investigation on performance of fins on a horizontal base in free convection heat transfer. J. Heat Mass Transfer Vol. 33 (1998).

[3] Yuncu and Yazicioglu, Optimum fin spacing of rectangular fins on a vertical base in free convection heat transfer..J. Heat Mass Transfer Vol. 44 (2007).

[4] Yuncu, Guvenc, An experimental investigation on performance of rectangular fins on a vertical base in free convection heat transfer. J. Heat Mass Transfer Vol. 37 (2001).

[5] Mobedi and Yuncu, A three dimensional numerical study on natural convection heat transfer from short horizontal rectangular fin array. J. Heat and Mass Transfer Vol. 39 (2003).

[6] Harahap and McManus, Natural convection heat transfer from horizontal rectangular fin array. J. Heat Transfer Vol. 89 (1967).

[7] Ranandan and Ramalingam, Thermal management of electronics: a review of literature. Thermal science Vol. 2 (2008).

[8] Elenbaas, Heat dissipation of parallel plates by free convection. J. Physica Vol. 9 (1942).

[9] Churchil, A comprehensive correlating equation for buoyancy-induced flow in channels, J. Letters in heat and mass transfer Vol. 4 (1977).

[10] Bar-Cohen and Rohsenow, Thermally optimum spacing of vertical, natural convection cooled, parallel plates. J. Heat Transfer Vol. 106 (1984).

[11] Culham, Yovanovich, and Lee, Thermal modeling of isothermal cuboids and rectangular heat sinks cooled by natural convection, IEEE transactions on components, J. packaging, and manufacturing technology Vol. 18 (1985).

[12] Bodoia and Ostrele, The development of free convection between heated vertical plates, ASME journal of heat transfer Vol. 84 (1962).

[13] Ofi and Hetherington, Application of the finite element method to natural convection heat transfer from the open vertical channel Int. J. Heat Mass Transfer (1977).

[14] Starner, McManus, An experimental investigation of free convection heat transfer from rectangular fin arrays. J. Heat Transfer Vol. 89 (1967).

[15] Welling, Woolridge Free-convection heat transfer coefficient from rectangular vertical fins. J. HeatTransfer Vol. 87 (1965).

[16] Chaddock Free convection heat transfer from vertical rectangular fin arrays. ASHRAE J Vol. 12 (1970).

[17] Aihara Natural convection heat transfer from vertical rectangular-fin arrays (part 2, heat transfer from fin-edges). Bull JSME Vol. 13 (1970).

[18] Aihara Natural convection heat transfer from vertical rectangular-fin arrays (part 3, heat transfer from fin-flats). Bull JSME Vol. 13 (1970).

[19] Leung, Probert, Shilton Heat exchanger: optimal separation for vertical rectangular fins protruding from a vertical rectangular base. J. Appl Energy Vol. 19 (1985).

[20] Leung, Probert, Shilton , Heat exchanger design: optimal uniform separation between rectangular fins protruding from a vertical rectangular base. J. Appl Energy Vol. 19 (1985).

[21] Leung, Probert, Shilton , Heat exchanger design: thermal performances of rectangular fins protrudingfrom a vertical or horizontal rectangular base. J. Appl Energy Vol. 20 (1985).

[22] Leung, Probert, Shilton, Heat transfer performance of vertical rectangular fins protruding from bases: effect of fin length. J. Appl Energy Vol. 22 (1986).

[23] Leung, Probert, Natural-convective heat exchanger with vertical rectangular fins and base: design criteria. ProcInstrMechEngrs Vol. 201 (1987).

[24] Leung, Probert, Heat exchanger performance: effect of orientation. Appl Energy, Vol. 33 (1989).

[25] Leung, Probert Thermal effectiveness of short protrusion rectangular heat exchanger fins. J. Appl Energy Vol. 34 (1989).

[26] Van de pol,. Tierney, Free convective heat transfer from vertical fin arrays, J. Transactions on parts, hybrid and packaging Vol. 10 (1974).

[27] Edwards, Chaddock, An experimental investigation of the radiation and free convection heat transfer from a cylindrical disk extended surface, Trans. Am. Soc. Heat. Refrig. Air-condit.Eng. Vol. 69 (1963).

[28] Chaddock, Freeconvection heat transfer from vertical fin arrays, ASHRAE J. 12 (1970).

[29] Sparrow, Acharya, A natural convection fin with a solution— determined nonmonotonically varying heat transfer coefficient, ASME J. Heat Transfer, Vol. 105 (1981).

[30] Saikhedkar, Sukhatme, Heat transfer from rectangular cross-sectioned vertical fin arrays, in: Proceedings of the sixth national heat and mass transfer conference, HMT(1981).

[31] Sparrow, Vemuri, Natural convection–radiation heat transfer from highly populated pin –fin arrays, ASME J. Heat Transfer, Vol. 107 (1985).

[32] Sparrow, Vemuri, Orientation effects on natural convective/ radiation pin-fin arrays, Int. J. Heat Mass Transfer 29 (1986).

[33] Azarkish, Sarvari, Behzadmehr, Optimum geometry design of a longitudinal fin with volumetric heat generation under the influences of natural convection and radiation, J. Energy Conversion and Management, Vol. 51 (2010).

[34] Rao, Naidu, Rao, Sharma, Heat transfer from a horizontal fin array by natural convection and radiation—A conjugate analysis, International Journal of Heat and Mass Transfer, Vol. 49 (2006).

[35] A. Bejan, Convection Heat Transfer, Wiley, New York, 1984

[36] Tamayol, Mcgregor, Demian, Trandafir, Bowler, Rada, Bahrami, Assessment of thermal performance of electronic enclosures with rectangular fins: A passive thermal solution (2011).

[37] Aihara, Maruyama, Free convective/radiative heat transfer from pin-fin arrays with a vertical base plate (general representation of heat transfer performance), Int Journal of heat and mass transfer, Vol. 33 (1989).

[38] ANSYS Fluent (ver. 12.1.4) Computational fluid dynamics softrware, ANSYS, Inc. Academic.

[39] Taylor, An Introduction to Error Analysis: The Study of Uncertainties in Physical Measurements, University Science Books, 199